

Thioether Bonded Nickel(II)-Azoimidazole Complexes: Structures, Spectra and Electrochemical Oxidation to the Nickel(III) State

Soumendranath Nandi,^[a] Debashis Bannerjee,^[a] Jian-Sung Wu,^[b] Tian-Huey Lu,^[b] Alexandra M. Z. Slawin,^[c] John Derek Woollins,^[c] Joan Ribas,^[d] and Chittaranjan Sinha*^[a]

Keywords: Nickel / Electrochemistry / Magnetic properties / Ferromagnetic coupling / Density functional calculations

Nickel(II) complexes of 1-alkyl-2-[(*o*-thioalkyl)phenylazo]imidazole (SRaaiNR') are described in this article. SRaaiNR' has imidazole-N, azo-N and thioether-S donor centres. Counter ions ClO₄⁻, pseudohalides [azide (N₃⁻), thiocyanate (CNS⁻)] are used in the syntheses of complexes. One of the structures of [Ni(SRaaiNR')₂](ClO₄)₂ has suggested meridional binding of tridentate chelator with *cis-trans-cis* configuration in the sequence of *cis*-N(imidazole), *trans*-N(azo) and *cis*-S(thioether). Structural study of Ni^{II}-azido-SRaaiNR' de-

finies $\mu_{1,1}$ -N₃ bridged Ni^{II} dimer, [Ni(NNS)(N₃)₂]₂ and thus show interesting intramolecular ferromagnetic coupling. The best fit gave the results: $J = 38.13 \pm 0.6 \text{ cm}^{-1}$, $g = 2.24 \pm 0.002$, $D = 8.1 \pm 0.4 \text{ cm}^{-1}$ and $R = 2.1 \times 10^{-4}$. DFT computation has attempted to explain spectral, redox and magnetic properties of the complexes.

(© Wiley-VCH Verlag GmbH & Co. KGaA, 69451 Weinheim, Germany, 2009)

1. Introduction

The coordination chemistry of N,S donor ligands have received great attention for their stability, chemical and electrochemical activities, and biological relevance.^[1,2] Thioether (-SR) forms very stable complexes with soft metal ions and has been employed in analytical chemistry for the extraction of toxic heavy metals like Cd^{II}, Hg(II/I), Pb^{II} etc.^[3] Design of ligands with thioether donor center in a chelated environment with N and/or O donors in which one of N centres is coming from imidazole is important in coordination chemistry to synthesise good working models,^[4–8] in view of their soft-hard character, excited state properties, chemoselective organic transformation, generation of anticancer drugs with reduced nephrotoxicity, regulatory transcription ability etc. The use of imidazolyl based polychelate or bulky ligands having N_xS_y donor centres has been of continuing interest.^[1,2] We have synthesized thioether functionalized azoimidazoles, 1-alkyl-2-[(*o*-thioalkyl)phenylazo]imidazoles (SRaaiNR') (**1**, **2**), where the donor centres are imidazole-N, azo-N and thioether-S.^[9] Nickel(II) complexes of SRaaiNR' are reported in this work. The counterions

like, ClO₄⁻, bridging anions like azide (N₃⁻), thiocyanate (CNS⁻) are used in the syntheses of complexes. The structures are confirmed by single-crystal X-ray diffraction study in representative cases. Electronic structure, spectra, redox and magnetic properties are explained by DFT calculation of optimized geometry of the complexes.

2. Results and Discussion

2.1. Synthesis and Formulation

Imidazolylazothioether (**1**) is generally a tridentate imidazole-N (N), azo-N (N'), thioether-S donor ligand.^[9] They are synthesized by coupling *o*-(thioalkyl)phenyldiazonium ions with imidazole in aqueous sodium carbonate solution and purified by solvent extraction and chromatographic process.

The alkylation is carried out by adding alkyl iodide (MeI, EtI) in dry THF solution to the corresponding 2-[(*o*-thioalkyl)phenylazo]imidazole in the presence of sodium hydride. They are abbreviated as SRaaiNR' (**1**).

The reaction between methanolic solution of Ni(ClO₄)₂·6H₂O and appropriate ligand, SRaaiNR' in 1:2 mol ratio has isolated shining dark crystals upon slow evaporation. The composition of the complex, [Ni(SRaaiNR')₂](ClO₄)₂ (**2**) is supported by microanalytical data. Upon addition of aqueous solution of NaN₃ or NH₄CNS (2 equiv.) to the mixture of NiCl₂ and SRaaiNR' (1:1 mol ratio) in MeOH has isolated brown-yellow crystalline compound. The composition is established as [Ni(SRaaiNR')(X)₂]₂ {Scheme 1 X = N₃⁻ (**3**) and CNS⁻ (**4**)}. The complexes are sufficiently soluble in common organic solvents viz., methanol, etha-

[a] Inorganic Chemistry Section, Department of Chemistry, Jadavpur University, Kolkata 700032, India
Fax: +91-033-2413-7121
E-mail: c_r_sinha@yahoo.com

[b] Department of Physics, National Tsing-Hua University, Hsinchu-300, Taiwan, ROC

[c] Department of Chemistry, University of St Andrews, St Andrews, Fife KY16 9ST, UK

[d] Departament de Química Inorgànica, Universitat de Barcelona, Diagonal 6487, 08028 Barcelona, Spain

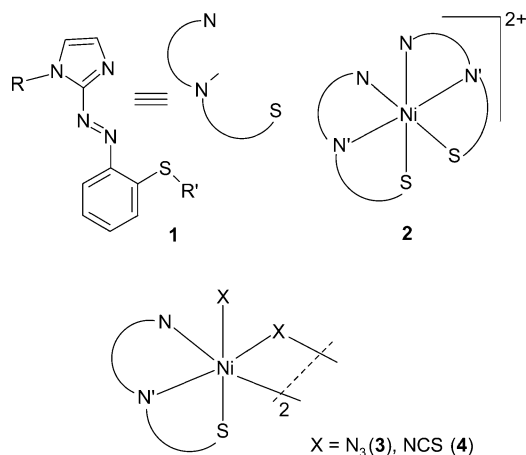
Supporting information for this article is available on the WWW under <http://dx.doi.org/10.1002/ejic.200900423>.

Table 1. UV/Vis spectral^[a] and magnetic moment data.

Compounds	UV/Vis Spectra in MeOH, λ_{max} [nm] (ϵ in $\text{dm}^3\text{mol}^{-1}\text{cm}^{-1}$)	Magnetic moment μ (BM)
[Ni(SMeaiiNMe) ₂](ClO ₄) ₂ (2a)	502 (3611), 459 (19355) ^[b] , 414 (28064), 356 (40000)	3.07
[Ni(SMeaiiNEt) ₂](ClO ₄) ₂ (2b)	503 (3085), 462 (14286) ^[b] , 413 (21714), 356 (31714)	2.80
[Ni(SETaaiNMe) ₂](ClO ₄) ₂ (2c)	509 (2706), 463 (17073) ^[b] , 413 (23171), 356 (33171)	2.73
[Ni(SETaaiNEt) ₂](ClO ₄) ₂ (2d)	508 (3288), 461 (23750) ^[b] , 419 (27500), 359 (31528)	3.02
[Ni(SMeaiiNMe)(N ₃) ₂] (3a)	619 (330), 456 (11833) ^[b] , 414 (18500), 369 (23167), 267 (14417)	2.08 ^[c]
[Ni(SMeaiiNEt)(N ₃) ₂] (3b)	620 (363), 457 (17105) ^[b] , 412 (27105), 369 (32763), 268 (21184)	2.17 ^[c]
[Ni(SETaaiNMe)(N ₃) ₂] (3c)	610 (1914), 457 (10276) ^[b] , 413 (15310), 370 (18414), 269 (12621)	2.18 ^[c]
[Ni(SETaaiNEt)(N ₃) ₂] (3d)	620 (919), 458 (10500) ^[b] , 411 (17300), 369 (20900), 267 (13600)	2.11 ^[c]
[Ni(SMeaiiNMe)(CNS) ₂] (4a)	650 (41), 463 (11834) ^[b] , 412 (17666), 358 (23000)	2.32 ^[c]
[Ni(SMeaiiNEt)(CNS) ₂] (4b)	651 (57), 461 (9143) ^[b] , 414 (13000), 362 (16286)	2.27 ^[c]
[Ni(SETaaiNEt)(CNS) ₂] (4c)	619 (62), 465 (6081) ^[b] , 414 (9865), 359 (13514)	2.18 ^[c]
[Ni(SETaaiNMe)(CNS) ₂] (4d)	650 (373), 460 (15250) ^[b] , 420 (19250), 365 (20750)	2.25 ^[c]

[a] In MeCN. [b] Shoulder. [c] Moment per Ni^{II}.

nol, chloroform, dichloromethane, acetonitrile but insoluble in hydrocarbons (hexane, benzene, toluene). They are non-conducting in methanol/acetonitrile solution. The complexes **2** show 1:2 molar conductivity ($\Lambda_{\text{M}} = 160\text{--}170 \text{ } \Omega^{-1} \text{ cm}^2 \text{ mol}^{-1}$ in MeOH) while **3** and **4** are non-electrolyte. At room temperature the effective magnetic moments (μ) of **2** lie 2.7–3.1 BM while **3** and **4** exhibit μ in the range of 2.0 to 2.3 BM. Magnetic moment of **2** lies in normal range of d⁸ electronic configuration to mononuclear Ni^{II} system while the reduced moment in the case of **3** and **4** may be due to spin exchange via Ni–(N₃)–Ni (**3**)/Ni–(NCS)–Ni (**4**) motif (Table 1).



Scheme 1. R = R' = Me (**1a**); R = Et, R' = Me (**1b**); R = Me, R' = Et (**1c**); R = R' = Et (**1d**); [Ni(NN'S)₂]²⁺ (**2**); [Ni(NN'S)(X)] (μ -X) {X = N₃ (**3**); CNS (**4**)}.

2.2. Spectral Studies

Infrared spectra of the complexes exhibit $\nu(\text{N}=\text{N})$ and $\nu(\text{C}=\text{N})$ at 1420–1430 and 1570–1590 cm^{-1} , respectively, and is red-shifted by 10 cm^{-1} relative to free ligand data.^[9] This supports coordination of azo-N and imine-N to Ni^{II}. The characteristic strong transmission of **3** at 2048–2055 and 2090–2105 cm^{-1} are referred to $\nu(\text{N}_3)$ and of **4** at 2080–2095 and 2100–2123 cm^{-1} are corresponding to $\nu_{\text{asym}}(\text{CNS})$. The presence of doublet pattern of splitting suggests two

different types of groups, bridging and terminal pseudohalides (N₃[−], NCS[−]).^[10,11] The $\nu(\text{ClO}_4)$ appears at 1090–1110 cm^{-1} (very strong) and 625–635 cm^{-1} (weak) stretching.

The electronic spectra of the complexes exhibit high intense transitions ($\epsilon \approx 10^4 \text{ M}^{-1} \text{ cm}^{-1}$) at 357 and 413 nm those are assigned to ligand centred $\pi\text{--}\pi^*$ and $n\text{--}\pi^*$ transitions, respectively. In the complexes **2** additional intense transitions appear at 460 and 505 nm along with shorter wavelength transition of free ligands. These transitions may be assigned $d\pi(\text{Ni})\text{--}\pi^*(\text{ligand})$, MLCT transitions (Table 1, Figure 1). The thioalkyl (–SR) group enhances the probability of charge transfer by MLCT path.^[2] [Ni–(SRaaiNR')(X)₂] {X = N₃[−] (**3**) and NCS[−] (**4**)} show additional weak transition at 620–650 nm along with transitions of complexes **2**.

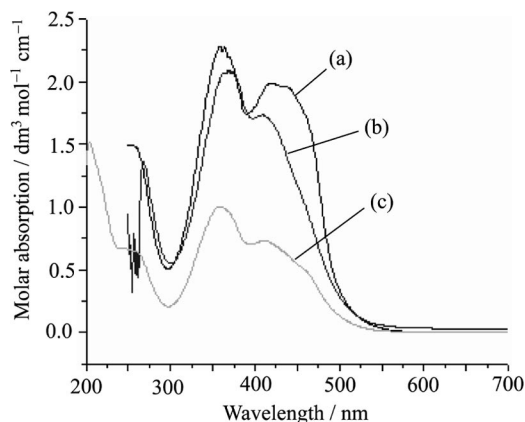


Figure 1. UV/Vis spectra of [Ni(SETaaiNEt)₂](ClO₄)₂ (a)(black line), [Ni(SETaaiNEt)($\mu_{1,1}$ -N₃)(N₃)₂] (b)(red line) and [Ni(SETaaiNEt)(CNS)₂] (c)(green line) in acetonitrile.

2.3. Molecular Structures

2.3.1. [Ni(SETaaiNEt)₂](ClO₄)₂ (**2d**)

The X-ray structure of [Ni(SETaaiNEt)₂](ClO₄)₂ (**2d**) is shown in Figure 2. Selected bond lengths and angles are given in Table 2. The coordination environment around

nickel in the complex is octahedral, NiN_4S_2 . The ligand SETaaiNEt acts as tridentate $\text{N}, \text{N}', \text{S}$ donor system (N refers to the imidazole nitrogen atom, N' refers to the azo N, and S refers to thioether S–Et donor centres). Metric parameters (Table 2) suggest distorted octahedral geometry around Ni centre. The coordination of two $\text{N}, \text{N}', \text{S}$ ligands shows *cis-trans-cis* arrangement in the sequence of N, N; N', N' ; S, S donor pairs and supports meridional configuration. Each $\text{Ni}(\text{N}, \text{N}', \text{S})$ fragment is planar (mean deviation $< 0.05 \text{ \AA}$). Ni^{II} moves upward from the reference square plane (ca. 0.04 \AA) constituted of N(2), N(5), N(3), S(2) atoms.

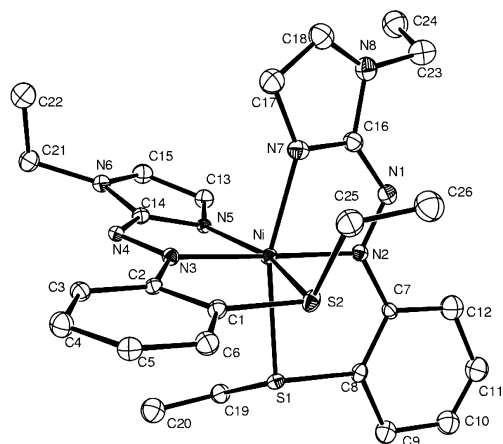


Figure 2. ORTEP view of $[\text{Ni}(\text{SETaaiNEt})_2](\text{ClO}_4)_2$ (**2d**) (hydrogen atoms are omitted for clarity).

The Ni–N distances vary in the range of $2.01\text{--}2.05 \text{ \AA}$. The distances are comparable with the structure of $[\text{Ni}(\text{MeaaiMe})(\text{NCS})_2(\text{H}_2\text{O})_2]$.^[12] The Ni–S distances [$\text{Ni}(\text{S}(1/2): 2.4429(16)/2.4328(19) \text{ \AA}$] also lie in the range of known Ni–S(thioether) chelated structures.^[2] The N=N distances differ significantly in two $\text{Ni}(\text{N}, \text{N}', \text{S})$ motifs [N(1)–N(2), $1.255(8)$; N(3)–N(4), $1.289(6) \text{ \AA}$]. The square plane, N(2), N(5), N(3), S(2), is constituted including N(3)–N(4) {azo function of $\text{Ni}[\text{N}(5), \text{C}(14), \text{N}(4), \text{N}(3)$ chelate]} in the equatorial plane whereas N(7) of $\text{Ni}[\text{N}(2), \text{N}(7)]$ chelate is in axial position that is bringing N(1)–N(2) {azo function of $\text{Ni}[\text{N}(2), \text{C}(16), \text{N}(1), \text{N}(7)$ chelate]} in the axial mode. The axial-equatorial distinction of two azo units may be the reason for difference in bond length.^[13,14]

Two chelate planes [Ni, S(1), C(8), N(2), deviation $\leq 0.1 \text{ \AA}$; Ni, N(7), C(16), N(1), N(2), mean deviation $\leq 0.07 \text{ \AA}$] per $\text{Ni}(\text{N}, \text{N}', \text{S})$ unit are almost planar and makes dihedral $4.5(2)^\circ$. The azoimine-chelated motif $\{-\text{Ni}(\text{N}=\text{N}=\text{C}=\text{N}^-)(\text{N}i-\text{N}')\}$ forms a better plane than the thioazo chelating unit $\{-\text{Ni}(\text{S}=\text{C}=\text{C}=\text{N}^-)(\text{N}i-\text{N}')\}$. The chelate angles $\text{Ni}(\text{N}, \text{N}')$ [$\angle \text{N}(2)\text{--Ni--N}(7)$, $77.7(2)^\circ$ and $\angle \text{N}(3)\text{--Ni--N}(5)$, $77.70(19)^\circ$] are smaller than for $\text{Ni}(\text{N}', \text{S})$ [$\angle \text{S}(1)\text{--Ni--N}(2)$, $81.72(15)^\circ$ and $\angle \text{S}(2)\text{--Ni--N}(3)$, $81.55(15)^\circ$] chelate. Large size of thioether–S may be the reason for such angular change which may lead to structural distortion.

$[\text{Ni}(\text{SETaaiNEt})_2]^{2+}$ and ClO_4^- are interacting through some hydrogen bonds with imidazole C–H of chelated ligand and forms 1-D chain. The supramolecular parameters

Table 2. Bond lengths and bond angles of $[\text{Ni}(\text{SETaaiNEt})_2](\text{ClO}_4)_2$ (**2d**) and $[\text{Ni}(\text{SMeaaiNEt})(\mu_{1,1}\text{-N}_3)(\text{N}_3)]_2$ (**3b**).

Bond length [Å]		Bond angles [°]	
[Ni(SEtaaiNEt) ₂](ClO ₄) ₂ (2d)			
Ni–N(3)	2.015(5)	N(3)–Ni–N(2)	177.1(2)
Ni–N(2)	2.032(5)	N(3)–Ni–N(7)	101.3(2)
Ni–N(7)	2.036(6)	N(2)–Ni–N(7)	77.7(2)
Ni–N(5)	2.049(4)	N(3)–Ni–N(5)	77.70(19)
Ni–S(2)	2.4328(19)	N(2)–Ni–N(5)	99.49(18)
Ni–S(1)	2.4429(16)	N(7)–Ni–N(5)	87.9(2)
N(1)–N(2)	1.255(8)	N(3)–Ni–S(2)	81.55(15)
N(3)–N(4)	1.289(6)	N(2)–Ni–S(2)	101.27(14)
		N(7)–Ni–S(2)	97.43(17)
		N(5)–Ni–S(2)	159.22(13)
		N(3)–Ni–S(1)	99.39(14)
		N(2)–Ni–S(1)	81.72(15)
		N(7)–Ni–S(1)	159.4(2)
		N(5)–Ni–S(1)	97.12(13)
		S(2)–Ni–S(1)	84.97(6)
[Ni(SMeaaiNEt)(μ _{1,1} -N ₃)(N ₃) ₂] (3b)			
Ni(1)–N(7)	2.060(3)	N(7)–Ni(1)–N(24)	99.22(13)
Ni(1)–N(24)	2.068(3)	N(7)–Ni(1)–N(21)#1	168.51(10)
Ni(1)–N(21)	2.085(3)	N(24)–Ni(1)–N(21)	92.20(13)
#1		#1	
Ni(1)–N(1)	2.090(3)	N(7)–Ni(1)–N(1)	77.30(10)
Ni(1)–N(21)	2.136(3)	N(24)–Ni(1)–N(1)	93.25(12)
Ni(1)–S(9)	2.4705(9)	N(21)#1–Ni(1)–N(1)	103.43(11)
N(6)–N(7)	1.277(4)	N(7)–Ni(1)–N(21)	89.29(10)
N(21)–N(22)	1.211(4)	N(24)–Ni(1)–N(21)	171.41(13)
N(21)–Ni(1)	2.085(3)	N(21)#1–Ni(1)–	79.27(11)
#1		N(21)	
N(22)–N(23)	1.153(4)	N(1)–Ni(1)–N(21)	89.78(10)
N(24)–N(25)	1.022(4)	N(7)–Ni(1)–S(9)	80.94(7)
N(25)–N(26)	1.239(5)	N(24)–Ni(1)–S(9)	95.92(10)
N(31)–C(32)	1.465(17)	N(21)#1–Ni(1)–S(9)	96.74(8)
#2			
		N(1)–Ni(1)–S(9)	157.48(8)
		N(21)–Ni(1)–S(9)	84.16(7)
		N(24)–N(25)–N(26)	176.7(4)

Symmetry transformations used to generate equivalent atoms

#1 $-x + 2/3, -y + 1/3, -z + 4/3$ #2 $-x + y, -x, z$ #3 $-y, x - y, z$

are as follows: C(13)–H(13)···O(1): H(13)···O(1), 2.45 \AA ; C(13)···O(1), 3.3509 \AA and $\angle \text{C}(13)\text{--H}(13)\cdots\text{O}(1)$, 163° . C(15)–H(15)···O(2₇): H(15)···O(2₇), 2.58 \AA ; C(15)···O(2₇), 3.2973 \AA and $\angle \text{C}(15)\text{--H}(15)\cdots\text{O}(2_7)$, 134° (symmetry: $3/2 - x, 1/2 + y, z$) C(17)–H(17)···O(5): H(17)···O(5), 2.31 \AA ; C(17)···O(5), 3.2265 \AA ; $\angle \text{C}(17)\text{--H}(17)\cdots\text{O}(5)$, 171° . C(18)–H(18)···O(8₆): H(18)···O(8₆), 2.31 \AA ; C(18)···O(8₆), 3.2158 \AA and $\angle \text{C}(18)\text{--H}(18)\cdots\text{O}(8_6)$, 163° (symmetry: $1/2 + x, y, 1/2 - z$). An intramolecular hydrogen bonding is observed with azo-N and imidazole–N(1)–CH₂ group C(23)–H(23A)···N(1)(Intra): H(23A)···N(1), 2.35 ; C(23)···N(1), 2.8384 ; $\angle \text{C}(23)\text{--H}(23A)\cdots\text{N}(1)$: 110° .

2.3.2. $[\text{Ni}(\text{SMeaaiNEt})(\mu_{1,1}\text{-N}_3)(\text{N}_3)]_2$ (**3b**)

The single-crystal structure of **3b** is shown in Figure 3. Selected bond lengths and angles are given in Table 2. The NiN_5S coordination sphere around Ni^{II} is distorted octahedral as can be seen from the angles subtended around the metal ion. The crystal structure carries one Et_3N in an isolated phase. The metric parameters in Et_3N are C–N,

1.466(2) Å and $\angle\text{C-N-C}$, 113.87(4)°. The SMeaiNEt binds as a tridentate N,N',S chelating fashion and the chelate angles are $\angle\text{N(7)-Ni(1)-N(1)}$, 77.30(10)° and $\angle\text{N(7)-Ni(1)-S(9)}$, 80.94(7)° those are comparable with reported values for other transition metal arylazo complexes [76.5° for a ruthenium(II) complex^[15] and 77.8° for a osmium(II) compound^[16]] and also with **2d**.

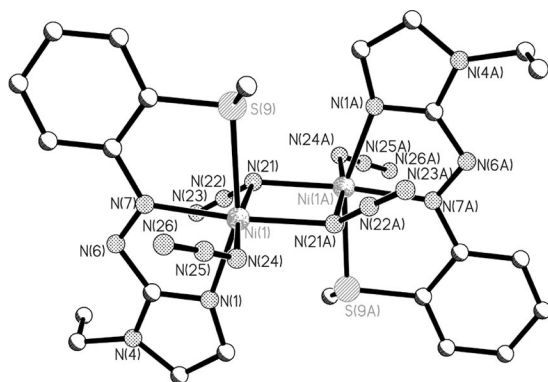


Figure 3. ORTEP view of $[\text{Ni}(\text{SMeaiNEt})(\mu_{1,1}\text{-N}_3)(\text{N}_3)_2]$ (**3b**).

One of N_3 -groups act as $\mu_{1,1}$ -bridger and other one is terminal. The bridging parallelogram is constructed by Ni_2N_2 [N(azido)] atoms participation. The bridge angles are $\text{Ni(1)-N(21)-Ni(1a)}$, 100.73(11)° and $\text{N(21)-Ni(1)-N(21a)}$, 79.27(11)°. The bridging arrangement, $\text{Ni(1)-N(21)-Ni(1a)-N(21a)}$ is planar. Two arms of Ni_2N_2 parallelogram are Ni(1)-N(21) , 2.136(3) and Ni(1)-N(21a) , 2.085(3) Å (symmetry: $-x + 2/3, -y + 1/3, -z + 4/3$). Terminal Ni-N(azido) distances, Ni(1/a)-N(24/24a) , 2.068(3) Å are shorter than bridged Ni-N(azido) [Ni(1)-N(21) , 2.136(3); Ni(1a)-N(21a) , 2.085(3) Å]. The N-N distances of $\mu_{1,1}$ -bridged azide are N(21)-N(22) , 1.211(4) and N(22)-N(23) , 1.153(4) Å while those of terminal azide are N(24)-N(25) , 1.022(4) and N(25)-N(26) , 1.239(5) Å. This reflects delocalized N(21)-N(22)-N(23) double bonding feature in the bridged azide group while terminal azide group [N(24)-N(25)-N(26)] shows higher bonding character than double bond in N(24)-N(25) and lower bonding feature than double bond in N(25)-N(26) . Terminal azide [N(24)-N(25)-N(26)] is slightly distorted from linearity [176.7(4)°] compared to $\mu_{1,1}$ -bridged azide [N(21)-N(22)-N(23) , 178.4(4)°]. Axial Ni-N_3 [N(24)-N(25)-N(26)] is no longer perpendicular on the square plane constituted by $\text{Ni(1), N(1), N(7), N(21a), S(9)}$ and is leaning towards Ni(1)-N(21a) side of bridging plane Ni_2N_2 [vide angles: $\text{N(21a)-Ni(1)-N(24)}$, 92.20(13) and N(7)-Ni(1)-N(24) , 99.22(13)°]. The Ni-N(azo) [Ni(1/a)-N(7/7a) , 2.060(3) Å] bond length is shorter than Ni-N(imidazole) distances [Ni(1/a)-N(1/a) , 2.090(3) Å] and reverse to the structural data of of $[\text{Ni}(\text{MeaiMe})(\text{NCS})_2(\text{H}_2\text{O})_2]$.^[12] This suggests the preference of azo-N to Ni^{II} in comparison with imidazole-N. This observation does not fit to our previous experience with 3d-group metal complexes of azoimidazoles. In Mn^{II} -azoimidazole-azido bridge the chelate, $\text{Mn}[\text{N(azo), N(imidazole)}]$ chelate that Mn-N(azo) (2.54 Å) is longer than Mn-N(imidazole) (2.203 Å);^[17,18] in $\text{Fe}[\text{N(azo), N(imidazole)}]$ unit

Fe-N(azo) (2.371 Å) > Fe-N(imidazole) (2.103 Å);^[12] $\text{Co}[\text{N(azo), N(imidazole)}]$ unit Co-N(azo) (2.328 Å) > Co-N(imidazole) (2.010 Å);^[19,20] $\text{Ni}[\text{N(azo), N(imidazole)}]$ unit Ni-N(azo) (2.252 Å) > Ni-N(imidazole) (2.052 Å);^[12,21] $\text{Cu}[\text{N(azo), N(imidazole)}]$ unit Cu-N(azo) (2.632 Å) > Cu-N(imidazole) (1.973 Å).^[9,22,23] The coordination of $-\text{S-R}$ may have influence on the strength of bonding interaction. Being a borderline acid Ni^{II} prefers to bind thioether-S that may assist $d\pi(\text{Ni}) \rightarrow \pi(\text{azo})$ charge flow and causes Ni-N(azo) bond contraction relative to Ni-N(imidazole) distance.

2.4. Metal Redox Behavior and Electro-Generation of Ni^{III} Species

Cyclic voltammetry is used to examine the redox behaviour of the complexes in acetonitrile/ CH_2Cl_2 solution. The complexes $[\text{Ni}(\text{N,N',S})_2]^{2+}$ (**2**) co-ordination sphere display a quasireversible (peak-to-peak separation 90–110 mV) one-electron cyclic response. Representative voltammogram is shown in Figure 4. All potentials are referred to the saturated calomel electrode (SCE). The potential (E) values as well as coulometric data confirming a one-electron stoichiometry are listed in Table 3. The redox behaviour at positive to SCE is metal centric (EPR evidence, see below) and can be represented as in Equation (1). The E , values of the couples lie in the range 0.75–0.85 V.

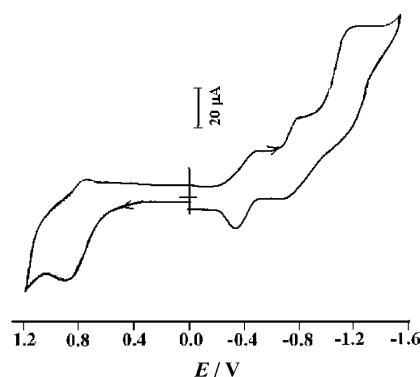


Figure 4. Cyclic voltammogram of $[\text{Ni}(\text{SEtaaiNEt})_2](\text{ClO}_4)_2$ in $\text{CH}_3\text{CN}/\text{CH}_2\text{Cl}_2$ solution mixture using Pt-working electrode, Pt-auxiliary electrode and SCE reference electrode in presence of $n\text{Bu}_4\text{N}^+ \text{ClO}_4^-$ as supporting electrolyte.

$\text{Ni}^{\text{III}}\text{-Ni}^{\text{II}}$ reduction potential data are known for a few complexes involving thioether co-ordination.^[1,2] The peak-to-peak separation of the couple is largely dependent on scan rate and increases from 130 mV at 50 mVs^{-1} to 400 mV at 1000 mVs^{-1} . At slow scan rates (20–50 mVs^{-1}) ΔE_p remains almost constant and also the E_{Pa} and the E_{Pc} values. This observation suggests low heterogeneous electron-transfer rate constant which has been influenced by the applied potential. This observation may reflect the change is geometry of the complex during redox transformation. Ni^{III} , being a hard acid centre, may develop strong covalent interac-

Table 3. Cyclic voltammetric data of the complexes.

Compound	Cyclic Voltammetry data ^[a] E [V], (ΔE [mV])	
	E_M	E_L
[Ni(SMeaaiNMe) ₂](ClO ₄) ₂ (2a)	0.82 (90)	−0.48 (120), −0.80 (140), −1.28 ^[b]
[Ni(SMeaaiNEt) ₂](ClO ₄) ₂ (2b)	0.76 (110)	−0.53 (110), −0.88 (160), −1.32 ^[b]
[Ni(SETaaiNMe) ₂](ClO ₄) ₂ (2c)	0.75 (100)	−0.52 (120), −0.84 (150), −1.28 ^[b]
[Ni(SETaaiNEt) ₂](ClO ₄) ₂ (2d)	0.80 (90)	−0.50 (120), −0.83 (140), −1.20 ^[b]
[Ni(SMeaaiNMe)(N ₃) ₂] ₂ (3a)	0.84 (120)	−0.38 (100), −0.76 (120), −1.28 ^[b]
[Ni(SMeaaiNEt)(N ₃) ₂] ₂ (3b)	0.82 (150)	−0.34 (150), −0.84 (150), −1.35 ^[b]
[Ni(SETaaiNMe)(N ₃) ₂] ₂ (3c)	0.85 (120)	−0.42 (110), −0.75 (140), −1.28 ^[b]
[Ni(SETaaiNEt)(N ₃) ₂] ₂ (3d)	0.88 (140)	−0.30 (130), −0.78 (160), −1.30 ^[b]
[Ni(SMeaaiNMe)(CNS) ₂] ₂ (4a)	0.69 (140)	−0.56 (170), −0.94 (150), −1.47 ^[b]
[Ni(SMeaaiNEt)(CNS) ₂] ₂ (4b)	0.66 (150)	−0.55 (160), −0.92 (160), −1.45 ^[b]
[Ni(SETaaiNMe)(CNS) ₂] ₂ (4c)	0.67 (160)	−0.55 (150), −0.90 (170), −1.48 ^[b]
[Ni(SETaaiNEt)(CNS) ₂] ₂ (4d)	0.64 (160)	−0.58 (150), −0.86 (160), −1.34 ^[b]

[a] Solvent MeCN/CH₂Cl₂ (3:1, v/v), Supporting electrolyte [nBu₄N](ClO₄), Pt-disk milli working electrode, Pt-wire auxiliary electrode, Reference electrode SCE, at 298 K, E_M = metal oxidation Ni^{III}/Ni^{II} couple, E_L = ligand reductions [−N=N−]/[−N=N−][−] and [−N=N−][−]/[−N=N−]^{2−} $E = 0.5 (E_{pa} + E_{pc})$ where E_{pa} is the anodic peak potential and E_{pc} is the cathodic peak potential, $\Delta E_p = |E_{pa} - E_{pc}|$. [b] E_{pc} .

tion with N(azo) and N(imidazole) centres while Ni^{II}, a borderline ion may strongly interact with S(thioether) and N(imidazole). Thus there will be a structural distortion on going from Ni(NNS)₂²⁺ to Ni(NNS)₂³⁺ in the electrochemical time scale. Chemical oxidation was tried with Ce^{IV} solution under heterogeneous phase (CH₂Cl₂/H₂O) and had been failed to isolate pure products. Reductive responses are observed at negative potential to reference potential; quasireversible couple at −0.3 to −0.5 V and −0.75 to −0.90 V may be the description of [−N=N−]/[−N=N−][−] and an irreversible response at −1.2 V is assigned to [−N=N−][−]/[−N=N−]^{2−} (Table 3).

Bluish-red solutions of thioether Ni^{III} species are produced upon coulometric oxidation (Table 2) of the corresponding Ni^{II} complexes in acetonitrile/CH₂Cl₂ solution. The tridentate nickel(III) complexes are thermally less stable and for these coulometry was performed at 258 K. Upon one-electron reduction of the oxidized solutions the original Ni^{II} species are regenerated. However, we could not be able to isolate Ni^{III} complexes in the solid state. Frozen solutions (77 K) of the Ni^{III} complexes display axial EPR spectra with $g_{\perp} \approx 2.15$ and $g_{\parallel} \approx 2.08$. A representative spectrum is shown in Figure 5, and spectral parameters are listed in Table 1. The g values lie predominantly metal [nickel(III), low-spin d⁷] orbital.^[2]

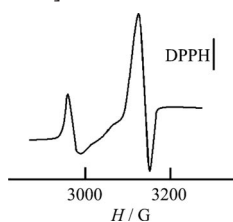


Figure 5. X-Band EPR of [Ni(SETaaiNEt)₂](ClO₄)₂ in frozen acetonitrile/CH₂Cl₂ solution ($G = 10^{-4}$ T).

2.5. Magnetic Property of Azido-Bridged [Ni(SMeaaiNEt)-(μ_{1,1}-N₃)(N₃)₂] (**3b**)

The magnetic properties of the complex **3b** in the form of $\chi_m T$ vs. T plot (χ_m is the molar magnetic susceptibility

for **3b** Ni^{II} ions) is shown in Figure 6 (top). The value of $\chi_m T$ at 300 K is 2.85 cm³ mol^{−1} K, a typical value for two nickel(II) ions with $g > 2.00$, as expected. Lowering the temperature there is a rapid increasing of $\chi_m T$ to 3.8 cm³ mol^{−1} K at ca 40 K and then a decrease to 2.6 cm³ mol^{−1} K at 2 K. These features indicate noticeable intramolecular ferromagnetic coupling with the presence of both weak intermolecular antiferromagnetic interactions and the effect of the single-ion zero field splitting (D parameter) of the Ni^{II} ions, always manifested at very low temperature.

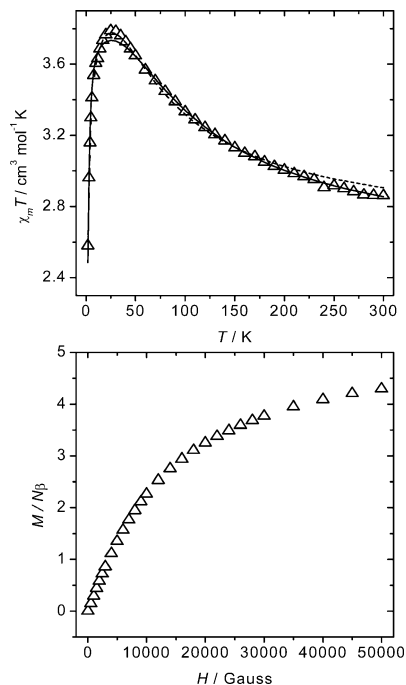


Figure 6. Top: Plot of the susceptibility data, $\chi_m T$ vs. T for **3b**. The solid line represents the best fit using the D parameter and the dotted line, with J' (see text for the explanation). Bottom: plot of the reduced magnetization, $M/N\beta$ vs. H data at 2 K.

As shown in the crystallographic part, complex **3b** (Figure 2) is made by Ni₂ dinuclear entities in which each Ni^{II} is linked by two azido in end-on coordination mode. The

fit of the $\chi_m T$ data has been made by two approaches: i) assuming *only* intermolecular antiferromagnetic interactions and applying the formula given by Kahn with the Hamiltonian $H = -J_i \sum S_i S_j$, introducing a J' parameter through the mean-field approach for calculating the intermolecular interactions.^[24,25] The best-fit parameters are: $J = 33.73 \pm 0.6 \text{ cm}^{-1}$, $g = 2.28 \pm 0.002$, $J' = -0.35 \pm 0.005 \text{ cm}^{-1}$ and $R = 2.4 \times 10^{-4}$ (R is the agreement factor defined as $\sum_i [(\chi_m T)_{\text{obs}} - (\chi_m T)_{\text{calc}}]^2 / \sum_i [(\chi_m T)_{\text{obs}}]^2$ (Figure 6); ii) the second approach was made by assuming that the decrease at low temperature is due only to the presence of the D parameter typical for Ni^{II} ions. In this case, a full diagonalization method was used, through a hand-made computer program.^[26] The best fit gave the following results: $J = 38.13 \pm 0.6 \text{ cm}^{-1}$, $g = 2.24 \pm 0.002$, $D = 8.1 \pm 0.4 \text{ cm}^{-1}$ and $R = 2.1 \times 10^{-4}$ (Figure 6). Considering that J' and D have the same effect on the curve of $\chi_m T$ at low temperature, any attempt to fit the experimental data with both parameters have no sense from chemical point of view. Thus, as a summary, J has a magnitude between +33 and +38 cm^{-1} and D is, likely, lower than the calculated value (ca. 8 cm^{-1}) due to the simultaneous effect of J' . Typical values of D for Ni^{II} complexes are close to 6 cm^{-1} .^[27] The plot of the reduced magnetization at 2 K is shown in Figure 6 bottom. The $M/N\beta$ value at saturation (5 T) is 4.4, in agreement with the presence of four electrons in the ground state.

The experimental reported complexes^[28] and theoretical studies^[29] have demonstrated that *almost* all dinuclear complexes with double azido ligand bridge in μ -1,1 coordination mode create ferromagnetic coupling. All data seem to

indicate that the main parameter is the M–N–M angle (N referring to N_3 bridging ligand). The Ni–N₃–Ni torsion (τ) angle seems to be less important in the magnitude of the J value. On the contrary, all experimental and theoretical calculations seem to indicate that for Ni^{II} systems the J value is always positive (ferromagnetic), for any value of Ni–N–Ni.^[29]

With respect to complex **3b**, the interaction is predicted to be ferromagnetic for all the range of Ni–N–Ni angles,^[29] with J increasing upon increasing this angle, yielding a maximum at $\theta \approx 104^\circ$. The Ni–N–Ni angle is 100.73° , very typical for this kind of systems. The Ni–N distances (2.085 and 2.136 Å) are very common and the torsion angle (very large) are less important than for copper(II) systems. The available structure shows a narrow range of θ value, and the experimental J values also vary little. The J value for **3b** lies, thus, between the typical ones reported in the literature.^[30]

2.6. DFT Computation and Correlation Structure, Spectra, Redox and Magnetic Properties of the Complexes

DFT calculation has been performed using the Gaussian03 (G03)^[31] software package. The Becke's three-parameter hybrid exchange functional and the Lee–Yang–Parr nonlocal correlation functional (B3LYP)^[32] were used for the calculation of two complexes $[\text{Ni}(\text{SEtaaiNet})_2](\text{ClO}_4)_2$ (**2d**) and $[\text{Ni}(\text{SMeaaiNet})(\mu_{1,1}\text{-N}_3)(\text{N}_3)]_2$ (**3b**). Elements except nickel were assigned a 6-31G* basis set. For nickel the Los Alamos effective core potential plus double

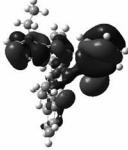
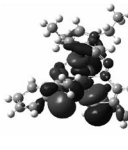
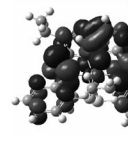
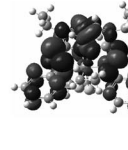
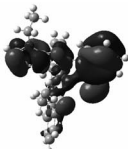
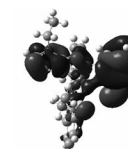

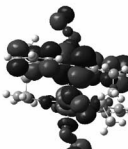
2d				
	HOMO-1 energy: -12.12 eV composition: Ni 9%, ligand 91%	HOMO energy: -10.69 eV composition: Ni 42%, ligand 58%	LUMO energy: -9.13 eV composition: Ni 4%, ligand 96%	LUMO+1 energy: -9.04 eV composition: Ni 3%, ligand 97%
3b				
	HOMO-1 energy: -4.51 eV composition: Ni 39%, ligand 25%, terminal N ₃ 32%, bridge N ₃ 4%	HOMO energy: -4.43 eV composition: Ni 35%, ligand 22%, terminal N ₃ 35%, bridge N ₃ 8%	LUMO energy: -3.51 eV composition: Ni 4%, ligand 91%, terminal N ₃ 5%	LUMO+2 energy: -2.79 eV composition: Ni 62%, ligand 11%, terminal N ₃ 11%, bridge N ₃ 16%

Figure 7. Surface plots of some of the MOs of **2d** and **3b** along with their energy and composition.

zeta (LanL2DZ)^[33] basis set was employed. The optimized structure of these molecules are developed using Gaussian 03 analyses package. The structural agreement has been observed from the comparison of bond lengths and angles between calculated and X-ray determined structures. The bond lengths of theoretically generated molecules are elongated by 0.01–0.03 Å than that of experimental structures. The calculated vibrational frequencies were red shifted by 5–10 cm^{−1} compared to the experimental result these ensured that optimized geometries represented local minima.

Theoretically generated structures are used to calculate composition and energy of the functions. These are used to explain the electronic properties of the complexes. The orbital energies along with contributions from the ligands and metal are given in the Supporting Information. The selected occupied and unoccupied frontier orbitals are shown in Figure 7. The MOs are destabilized on going from [Ni(SEtaaiNet)₂](ClO₄)₂ (**2d**) to [Ni(SMeaaiNet)(μ_{1,1}-N₃)(N₃)₂] (**3b**). E_{HOMO} (**2d**), −10.69 eV and E_{HOMO} (**3b**), −4.43 eV; E_{LUMO} (**2d**), −9.13 eV and E_{LUMO} (**3b**), −3.51 eV. This may be attributed from structural distortion, coordination of different donor centres, number of chelate rings etc.

GaussSum^[34] was used to calculate the fractional contributions of various groups to each molecular orbital. This is done using Mulliken population analysis.

The electronic structures of the complexes are characterized by high degree of mixing between Ni(dπ) and ligand-π/pπ orbitals. The HOMO of two structures in gas phase has >35% Ni contribution. In [Ni(SEtaaiNet)₂](ClO₄)₂ (**2d**) HOMO-1, HOMO-2 and lower occupied MOs have major participation of ligand orbitals. The HOMO-1 in [Ni(SMeaaiNet)(μ_{1,1}-N₃)(N₃)₂] (**3b**) is composed of Ni(dπ) (39%), terminal-N₃ (32%), bridge-N₃ (4%) and chelated ligand (25%) while HOMO-2 contains 95% terminal-N₃ functions. The LUMO and LUMO+1 are delocalized mainly SEtaaiNet or SMeaaiNet. The LUMO+2 has >60% Ni(dπ) functions.

The electronic absorption spectra are measured at room temperature in acetonitrile, and the experimental absorption bands are assigned using the singlet-excited states calculation. The calculated excitation wavelength and their assignment are given in Table 4. The intensity of these transitions has been assessed from oscillator strength (*f*). In **2d** the visible region (400–530 nm) transitions are assigned to

Table 4. Selected list of excited energies of of [Ni(SEtaaiNet)₂](ClO₄)₂ (**2d**) and [Ni(SMeaaiNet)(μ_{1,1}-N₃)(N₃)₂] (**3b**) in gas phase.

[Ni(SEtaaiNet) ₂](ClO ₄) ₂ (2d)			
Wavelength [nm]	Oscillator strength (<i>f</i>)	Major Transitions	Assignment ^[a]
529.46	0.0172	H-1→LUMO (80%)	ILCT
515.67	0.0159	H-2→LUMO (73%)	ILCT
456.78	0.0461	H-3→L+1 (34%)	ILCT
		H-6→LUMO (14%)	XLCT + MLCT
452.82	0.0419	H-2→L+1 (22%)	ILCT
		H-3→L+1 (15%)	ILCT
433.37	0.0414	H-6→LUMO (24%)	ILCT+MLCT
		H-5→LUMO (17%)	MLCT+ILCT
		H-4→LUMO (17%)	ILCT
403.63	0.1860	H-6→LUMO (25%)	ILCT+MLCT
		H-7→LUMO (12%)	ILCT+MLCT
394.70	0.2757	H-5→LUMO (26%)	MLCT+ILCT
		H-6→LUMO (15%)	ILCT+MLCT
371.02	0.0902	H-6→LUMO (45%)	ILCT+MLCT
366.23	0.0676	H-7→LUMO (22%)	ILCT+MLCT
		H-6→LUMO (32%)	ILCT+MLCT
340.73	0.0997	H-8→L+1 (38%)	ILCT
330.71	0.0356	H-1→L+2 (27%)	LMCT+ILCT
		H-10→LUMO (23%)	ILCT
306.68	0.0674	H-8→LUMO (38%)	ILCT
278.17	0.0124	H-11→LUMO (20%)	ILCT
		H-13→LUMO (17%)	ILCT+MLCT
[Ni(SMeaaiNet)(μ _{1,1} -N ₃)(N ₃) ₂] (3b)			
809.66	0.0022	H-6→LUMO (60%)	XLCT+MLCT
616.65	0.0168	H-5→L+1 (52%)	YLCT+MLCT+XLCT
538.19	0.2059	H-6→L+2 (34%)	XMCT+MMCT
		H-5→L+1 (24%)	YLCT+MLCT+XLCT
513.01	0.0288	H-7→L+2 (42%)	MMCT+XMCT
480.85	0.0438	H-7→L+2 (35%)	MMCT+XMCT
463.45	0.0185	H-10→LUMO (42%)	MLCT+MMCT
444.66	0.0025	H-1→L+3 (60%)	MMCT+MXCT+YMCT+YXCT+LMCT+LXCT
		H-2→L+3 (34%)	YLCT+YXCT

[a] M = metal, L = ligand, X = bridge azide, Y = terminal azide (MLCT: metal-to-ligand charge transfer; XLCT: bridge azide-to-ligand charge transfer; YLCT: terminal azide-to ligand charge transfer; ILCT: intraligand charge transfer; MMCT = metal to metal charge transfer etc., H = HOMO; L = LUMO).

HOMO→LUMO, HOMO-*n*→LUMO/LUMO+1 (*n* = 1 to 7). The transitions are weak (*f*, 0.01–0.04) and are assigned to admixture of MLCT (metal-to-ligand charge transfer) and ILCT (intraligand charge transfer). An intense band is calculated at 403 nm (*f*, 0.186) which is ILCT+MLCT band. [Ni(SMeaaiNEt)(μ_{1,1}-N₃)(N₃)₂] (3b) shows longer wavelength transition (>600 nm) but they are weak (*f*, 0.0022, 0.0168). They are assigned to the mixture of MLCT and N₃→SMeaaiNEt transition. Other transitions at shorter wavelength (530–300 nm) are mixture of MLCT, ILCT, MMCT, XMCT (X = azide) transitions.

The DFT computation of 3b shows that terminal-N₃ and bridge-N₃ contribute to MOs. Present calculation at room temperature can not fully account the intramolecular ferromagnetic coupling and weak intermolecular antiferromagnetic interactions but suggests the sharing of orbitals through Ni–N₃–Ni bridge. As Ni contributes significantly to filled (HOMO, HOMO-1) and vacant (LUMO+2) MOs, the effect of the single-ion zero field splitting (*D* parameter) of the Ni^{II} ions is adjusted at low temperature.

Conclusions

The Ni^{II} complexes of 1-alkyl-2-[(*o*-thioalkyl)phenylazo]-imidazoles are characterized in this work. The ligand belongs to N(imidazole), N(azo), S(thioether) tridentate donor system. The complexes of formulae [Ni(NN'S)₂](ClO₄)₂ and [Ni(NN'S)(X)₂]₂ (where X is bridging pseudo halogen, N₃ and NCS) are characterized by single-crystal X-ray diffraction studies. Azido bridge, [Ni(NNS)(N₃)₂]₂ complexes show interesting intramolecular ferromagnetic coupling. The complexes undergo electrooxidation affording EPR characterisable Ni^{III} species which have d_{z²} ground state. The electronic and magnetic properties are explained by DFT computation.

Experimental Section

Materials: NiCl₂·6H₂O, *o*-(amino)thiophenol, methyl iodide (MeI), ethyl iodide (EtI), NaN₃, NH₄CNS were purchased from E. Merck, India. Ni(ClO₄)₂·6H₂O was prepared from NiCO₃. Solvents were used after drying.^[35] All experiments were carried out under N₂ atmosphere. The syntheses of the ligands were carried out following common procedure^[9] of coupling *o*-(thioalkyl)phenyldiazonium ion [obtained by diazotization of *o*-(thioalkyl)aniline] with imidazole at pH 7 followed by N(1)-alkylation using alkyl iodide in presence of NaH in dry THF under dry and inert condition.

Physical Measurement: Microanalyses (C,H,N) were performed using a Perkin–Elmer 2400 CHNO/S elemental analyzer. Spectroscopic measurements were carried out using the following instruments: UV/Vis spectra, Perkin–Elmer UV/Vis Spectrophotometer model Lambda 25. IR spectra (KBr disk, 4000–400 cm^{−1}), PerkinElmer FT-IR Spectrophotometer model Spectrum RX1. Room temperature magnetic moment was measured using Magnetic Susceptibility Balance, Sherwood Scientific Cambridge, UK. Molar conductance (*A*_M) was measured in a Systronics conductivity meter 304 model using ca. 10^{−3} M solutions in MeOH. Electrochemical measurements were performed using computer-controlled PAR

model 250 VersaStat electrochemical instruments with Pt-disk electrodes. All measurements were carried out under nitrogen environment at 298 K with reference to SCE in acetonitrile using [*n*Bu₄N]·[ClO₄] as supporting electrolyte. The reported potentials are uncorrected for junction potential. EPR spectra were measured in MeCN/CH₂Cl₂ solution at room temperature (298 K) and liquid nitrogen temperature (77 K) using Bruker EPR spectrometer model EMX 10/12, X-band ER 4119 HS cylindrical resonator. Magnetic measurements on powdered samples were performed for the temperature range 2–300 K using a Quantum Design MPMS-7 SQUID magnetometer in a magnetic field of 0.1 T. The experimental susceptibilities were corrected for the diamagnetism of the constituent atoms (Pascal tables).

Synthesis of Complexes

[Ni(SMeaaiNMe)₂](ClO₄)₂ (2a): 1-Methyl-2-[*o*-(thiomethyl)phenylazo]imidazole (SMeaaiNMe) (0.4 g, 1.72 mmol) in methanol (10 mL) was added drop wise to a methanolic solution (10 mL) of Ni(ClO₄)₂·6H₂O (0.3 g, 0.82 mmol) at 298 K. Orange-brown solution was stirred for 10 min. It was then filtered and left undisturbed for a week. Dark crystalline compound was separated. The crystals were filtered, washed with water, cold methanol and dried with CaCl₂ in vacuo; yield 0.35 g (59%).

All other complexes were prepared by the same procedure. The yield varied from 50–70%.

Microanalytical Data: Fd (Calc.%) For [Ni(SMeaaiNMe)₂](ClO₄)₂ (2a): C, 36.64 (36.58); H, 3.27 (3.33); N, 15.45 (15.52). For [Ni(SMeaaiNEt)₂](ClO₄)₂ (2b): C, 38.50 (38.42); H, 3.70 (3.73); N, 14.85 (14.94). For [Ni(SETaaiNMe)₂](ClO₄)₂ (2c): C, 38.38 (38.42); H, 3.68 (3.73); N, 14.90 (14.94). For [Ni(SETaaiNEt)₂](ClO₄)₂ (2d): C, 40.00 (40.12); H, 4.05 (4.11); N, 14.33 (14.40%).

[Ni(SMeaaiNMe)(N₃)₂]₂ (3a): 1-Methyl-2-[*o*-(thiomethyl)phenylazo]imidazole (SMeaaiNMe) (0.2 g, 0.86 mmol) in methanol (10 mL) was added drop wise to a methanolic solution (10 mL) of NiCl₂·6H₂O (0.21 g, 0.88 mmol) at 298 K. Orange-brown solution was stirred for 10 min. To this solution NaN₃ (0.13 g, 2.00 mmol) was added in small volume of water. The resulting brown red solution was then filtered and left undisturbed for a week. Dark crystalline compound was separated. The crystals were filtered, washed with water, cold methanol and dried with CaCl₂ in vacuo; yield 0.22 g (56%).

All other complexes were prepared by the same procedure. The yield varied from 50–70%.

[Ni(SMeaaiNMe)(N₃)₂]₂ (3a): Microanalysis, found (calcd.): C 35.16 (35.23), H 3.13 (3.20), N 37.44 (37.36).

[Ni(SMeaaiNEt)(N₃)₂]₂ (3b): Microanalysis, found (calcd.): C 37.12 (37.05), H 3.53 (3.60), N 35.96 (36.02).

[Ni(SETaaiNMe)(N₃)₂]₂ (3c): Microanalysis, found (calcd.): C 37.10 (37.05), H 3.65 (3.60), N 36.00 (36.02).

[Ni(SETaaiNEt)(N₃)₂]₂ (3d): Microanalysis, found (calcd.): C 38.68 (38.74), H 3.93 (3.97), N 34.80 (34.77).

[Ni(SMeaaiNMe)(CNS)₂]₂: 1-Methyl-2-[*o*-(thiomethyl)phenylazo]imidazole (SMeaaiNMe) (0.2 g, 0.86 mmol) in methanol (10 mL) was added dropwise to a methanolic solution (10 mL) of NiCl₂·6H₂O (0.21 g, 0.88 mmol) at 298 K. Orange-brown solution was stirred for 10 min. To this solution NH₄NCS (0.15 g, 1.97 mmol) was added in small volume of water. The resulting brown-violate solution was then filtered and left undisturbed for a week. Dark crystalline compound was separated. The crystals were filtered, washed with water, cold methanol and dried with CaCl₂ in vacuo. Yield was 0.24 g, (64%).

All other complexes were prepared by the same procedure. The yields varied from 50–70%.

[Ni(SMeaiiNMe)(CNS)₂]₂ (4a): Microanalysis, found (calcd.): C 38.45 (38.36), H 3.03 (2.95), N 20.58 (20.65).

[Ni(SMeaiiNEt)(CNS)₂]₂ (4b): Microanalysis, found (calcd.): C 40.00 (39.93), H 3.30 (3.33), N 20.05 (19.97).

[Ni(SETaiiNMe)(CNS)₂]₂ (4c): Microanalysis, found (calcd.): C 40.03 (39.93), H 3.28 (3.33), N 20.10 (19.97).

[Ni(SETaiiNEt)(CNS)₂]₂ (4d): Microanalysis, found (calcd.): C 41.31 (41.41), H 3.64 (3.68), N 19.28 (19.32).

X-ray Crystal Structure Analysis: Details of crystal analyses, data collection and structure refinement are given in Table 5. Single crystal data collection were performed with Siemens SMART CCD area detector diffractometer using fine focus sealed graphite-monochromatized Mo- K_{α} radiation ($\lambda = 0.71073 \text{ \AA}$) for [Ni(SETaiiNEt)₂](ClO₄)₂ (**2d**). For [Ni(SMeaiiNEt)($\mu_{1,1}$ -N₃)(N₃)₂] (**3b**) data were collected using a Rigaku MM007 rotating anode/confocal optics (Mo- K_{α} radiation, $k = 0.71073 \text{ \AA}$) and a Mercury CCD at 93(2) K. Reflections were recorded using the ω scan technique. Data were corrected for Lorentz polarization and absorption effects and for linear decay. Semi-empirical absorption corrections based on ψ -scans were applied with the help of Bruker SAINT for **2d** and CrystalClear (Rigaku Corp., 2004) for **3b**. The structure was solved by direct methods using SHELXS-97^[36] and successive difference Fourier syntheses. All non-hydrogen atoms were refined anisotropically. In the final difference Fourier map the residual minima and maxima were $[-0.314, 0.615 \text{ (e/\AA}^3\text{)}]$ for **2d**; $[-0.341 \text{ and } 0.511 \text{ (e/\AA}^3\text{)}]$ for **3b** carried out using SHELXL-97^[37]. The structures were drawn by using ORTEP-32,^[38] and PLATON-99^[39] programs.

Table 5. Summarized crystallographic data for [Ni(SETaiiNEt)₂](ClO₄)₂ (**2d**) and [Ni(SMeaiiNEt)($\mu_{1,1}$ -N₃)(N₃)₂] (**3b**).

	2d	3b
Empirical formula	C ₂₆ H ₃₂ Cl ₂ N ₈ NiO ₈ S ₂	C ₂₆ H ₃₃ N _{20.33} Ni ₂ S ₂
Formula weight	778.33	811.93
Temperature /K	294(2)	93(2)
Crystal system	orthorhombic	rhombohedral
Space group	<i>Pbca</i>	<i>R</i> ₃
Crystal size /mm ³	0.20 × 0.20 × 0.20	0.20 × 0.10 × 0.05
<i>a</i> /Å	14.3482(9)	30.0835(12)
<i>b</i> /Å	14.5084(9)	30.0835(12)
<i>c</i> /Å	33.987(2)	10.6749(3)
β /°	90	90
γ /°		120°
<i>V</i> /Å ³	7075.1(8)	8366.6(5)
<i>Z</i>	8	9
μ (Mo- K_{α}) /mm ⁻¹	0.874	1.175
θ range	1.20–28.35	2.47 to 25.35°
<i>hkl</i> range	–19 ≤ <i>h</i> ≤ 11; –17 ≤ <i>k</i> ≤ 18; –42 ≤ <i>l</i> ≤ 42	0 ≤ <i>h</i> ≤ 34; –34 ≤ <i>k</i> ≤ 17; –9 ≤ <i>l</i> ≤ 12
<i>D</i> _{calc} /mgm ⁻³	1.461	1.450
Refine parameters	424	239
Total reflections	42182	12344
Unique reflections	8099	3188
<i>R</i> ₁ ^[a] [<i>I</i> > 2σ(<i>I</i>)]	0.0666	0.0372
<i>wR</i> ₂ ^[b]	0.2098	0.0865
Goodness of fit	0.631	1.057

[a] $R = \sum |F_o| - |F_c| / \sum |F_o|$. [b] $wR_2 = [\sum w(F_o^2 - F_c^2)^2 / \sum w(F_o^2)^2]^{1/2}$, $w = 1/[\sigma^2(F_o^2) + (0.3050P)^2]$ for **2d**; $w = 1/[\sigma^2(F_o^2) + (0.046P)^2 + (38.6183P)]$ for **3b** where $P = (F_o^2 + 2F_c^2)/3$.

CCDC-705025 (for **2d**) and -705026 (for **3b**) contain the crystallographic data for this article. These data can be obtained free of charge from the Cambridge Crystallographic Data Centre via www.ccdc.cam.ac.uk/data_request/cif.

Supporting Information (see footnote on the first page of this article): Selected list of excited energies of **2d** and **3b**; orbital contribution data of **2d** and **3b**.

Acknowledgments

Financial support from University Grants Commission, CAS-UGC, New Delhi are thankfully acknowledged. J. R. acknowledges the financial support given by the Spanish Government (Grant BQU2003-00539).

- [1] R. A. Allred, S. A. Hufner, K. Rudzka, A. M. Arif, L. M. Berreau, *Dalton Trans.* **2007**, 351–357; M. R. Malachonsk, M. Adams, N. Elia, A. L. Rheingold, R. S. Kelly, *J. Chem. Soc., Dalton Trans.* **1999**, 2177; B. Adhikary, S. Liu, C. R. Lucas, *Inorg. Chem.* **1993**, 32, 5957–5962.
- [2] K. Pramanik, S. Karmakar, S. B. Choudhury, A. Chakravorty, *Inorg. Chem.* **1997**, 36, 3562–3564; S. Mukhopadhyay, D. Ray, *J. Chem. Soc., Dalton Trans.* **1995**, 265–268; S. Karmakar, S. B. Choudhury, D. Ray, A. Chakravorty, *Polyhedron* **1993**, 12, 2325–2329; A. K. Singh, R. Mukherjee, *Dalton Trans.* **2005**, 2886–2891.
- [3] M. Matzapetakis, D. Ghosh, T. C. Weng, J. E. Penner-Hahn, V. L. Pecoraro, *Biol. Inorg. Chem.* **2006**, 11, 876–890; T. K. Ronson, H. Adams, L. P. Harding, R. W. Harrington, W. Clegg, M. D. Ward, *Polyhedron* **2007**, 26, 2777.
- [4] E. I. Solomon, R. K. Szilagy, S. D. George, L. Basumallick, *Chem. Rev.* **2004**, 104, 419–458; D. B. Rorabacher, *Chem. Rev.* **2004**, 104, 651; H. W. Yim, L. M. Tran, E. D. Dobbin, D. Rabinovich, L. M. Liablesands, C. D. Incarvito, K.-C. Larn, A. L. Rheingold, *Inorg. Chem.* **1999**, 38, 2211–2215.
- [5] P. Chakraborty, S. K. Chandra, A. Chakravorty, *Inorg. Chem.* **1994**, 33, 4959; P. Chakraborty, S. K. Chandra, A. Chakravorty, *Inorg. Chem.* **1993**, 32, 5349–5353; P. Chakraborty, S. K. Chandra, A. Chakravorty, *Organometallics* **1993**, 12, 4726; M. A. Bennell, L. Y. Goh, A. C. Willis, *J. Chem. Soc., Chem. Commun.* **1992**, 1180.
- [6] T. Shi, J. Berglund, L. I. Elding, *Inorg. Chem.* **1996**, 35, 3498; S. Choi, S. Mahalingaiah, S. Delaney, N. R. Neale, S. Massod, *Inorg. Chem.* **1999**, 38, 1800; M. D. Hall, T. W. Hambley, *Coord. Chem. Rev.* **2002**, 232, 49; E. Bouwman, W. L. Driessen, J. Reedijk, *Coord. Chem. Rev.* **1990**, 104, 143.
- [7] R. Balamurugan, M. Palaniandavar, R. S. Gopalan, G. U. Kul-karni, *Inorg. Chim. Acta* **2004**, 357, 919–930; M. Vidyanathan, R. Balamurugan, S. Usha, M. Palaniandavar, *J. Chem. Soc., Dalton Trans.* **2001**, 3498, and references cited therein.
- [8] B. C. Westerby, K. L. Juntunen, G. H. Leggett, V. B. Ptt, M. J. Koenigbauer, M. D. Rurgett, M. J. Jascher, L. A. Ochry-mow-yez, D. B. Rorabacher, *Inorg. Chem.* **1991**, 30, 2109; K. K. Nanda, A. W. Addison, R. J. Butcher, M. R. McDevitt, T. N. Rao, E. Sinn, *Inorg. Chem.* **1997**, 36, 134–135.
- [9] D. Banerjee, U. S. Ray, S. Jasimuddin, J.-C. Liou, T.-H. Lu, C. Sinha, *Polyhedron* **2006**, 25, 1299–1306.
- [10] U. S. Ray, B. G. Chand, G. Mostafa, J. Chang, T.-H. Lu, C. Sinha, *Polyhedron* **2003**, 22, 2587–2594.
- [11] U. S. Ray, K. K. Sarker, G. Mostafa, T.-H. Lu, M. S. El Fallah, C. Sinha, *Polyhedron* **2006**, 25, 2764–2772.
- [12] D. Banerjee, U. S. Ray, J.-C. Liou, C.-N. Lin, T.-H. Lu, C. Sinha, *Inorg. Chim. Acta* **2005**, 358, 1019–1026.
- [13] J. E. Huheey, E. A. Keiter, R. L. Keiter, *Inorganic Chemistry*, 4th ed., Harper Collins (Addison-Wesley Publishing Company), Reading, MA, **2000**.
- [14] A. G. Orpen, L. Brammar, F. K. Allen, O. Kennard, D. G. Watson, R. Taylor, *J. Chem. Soc., Dalton Trans.* **1989**, S1.

- [15] A. Seal, S. Ray, *Acta Crystallogr., Sect. C: Struct. Commun.* **1984**, 40, 929.
- [16] B. K. Ghosh, A. Mukhopadhyay, S. Goswami, S. Ray, A. Chakravorty, *Inorg. Chem.* **1984**, 23, 4633.
- [17] U. S. Ray, B. K. Ghosh, M. Monfort, J. Ribas, G. Mostafa, T.-H. Lu, C. Sinha, *Eur. J. Inorg. Chem.* **2004**, 250–259.
- [18] P. Bhuina, U. S. Ray, G. Mostafa, J. Ribas, C. Sinha, *Inorg. Chim. Acta* **2006**, 359, 4660–4666.
- [19] D. Banerjee, C. Sinha, *Indian J. Chem. A* **2006**, 45, 2224–2228.
- [20] U. S. Ray, B. G. Chand, G. Mostafa, J. Chang, T.-H. Lu, C. Sinha, *Polyhedron* **2003**, 22, 2587–2594.
- [21] P. Bhunia, D. Sardar, K. K. Sarker, U. S. Ray, J.-S. Wu, T.-H. Lu, C. Sinha, *J. Coord. Chem.* **2009**, 62, 552–563.
- [22] U. S. Ray, K. K. Sarker, G. Mostafa, T.-H. Lu, M. S. El Fallah, C. Sinha, *Polyhedron* **2006**, 25, 2764–2772.
- [23] U. S. Ray, D. Banerjee, G. Mostafa, T.-H. Lu, C. Sinha, *New J. Chem.* **2004**, 28, 1432–1437.
- [24] B. Bleaney, K. D. Bowers, *Proc. Roy. Soc. (London) Ser. A* **1952**, 214, 451.
- [25] O. Kahn, *Molecular Magnetism*, VCH Publishers, New York, **1993**.
- [26] This program was kindly supplied by Dr. Vassilis Tangoulis from the University of Patras (Greece).
- [27] R. Boca, *Struct. Bonding (Berlin)* **2006**, 117, 1, and references cited therein.
- [28] J. Ribas, A. Escuer, M. Monfort, R. Vicente, R. Cortés, L. Lezama, T. Rojo, *Coord. Chem. Rev.* **1999**, 193–195, 1027, and references cited therein.
- [29] E. Ruiz, J. Cano, S. Alvarez, P. Alemany, *J. Am. Chem. Soc.* **1998**, 120, 11122, and references cited therein.
- [30] S. S. Tandon, L. K. Thompson, M. E. Manuel, J. N. Bridson, *Inorg. Chem.* **1994**, 33, 5555.
- [31] M. J. Frisch, G. W. Trucks, H. B. Schlegel, P. M. W. Gill, B. G. Johnson, M. A. Robb, J. R. Cheeseman, T. A. Keith, G. A. Petersson, J. A. Montgomery, K. Raghavachari, M. A. Al-Laham, V. G. Zakrzewski, J. V. Ortiz, J. B. Foresman, J. Cioslowski, B. B. Stefanov, A. Nanayakkara, M. Challacombe, C. Y. Peng, P. Y. Ayala, W. Chen, M. W. Wong, J. L. Andres, E. S. Replogle, R. Gomperts, R. L. Martin, D. J. Fox, J. S. Binkley, D. J. Defrees, J. Baker, J. P. Stewart, M. Head-Gordon, C. Gonzalez, J. A. Pople, *Gaussian98*; Gaussian, Inc., Pittsburgh, PA, **1998**.
- [32] C. Lee, W. Yang, R. G. Parr, *Phys. Rev. B* **1988**, 37, 785.
- [33] P. J. Hay, W. R. Wadt, *J. Chem. Phys.* **1985**, 82, 270.
- [34] N. M. O'Boyle, J. G. Vos, *GaussSum 1.0*, Dublin City University, Dublin, Ireland, **2005**. Available from <http://gausssum.sourceforge.net>.
- [35] A. I. Vogel, *A Text Book of Practical Organic Chemistry*, **1959**, 2nd ed., Longman, London.
- [36] G. M. Sheldrick, *SHELXS-97, Program for the Solution of Crystal Structure*, University of Göttingen, Germany, **1997**.
- [37] G. M. Sheldrick *SHELXL 97, Program for the Refinement of Crystal Structure*, University of Göttingen, Germany, **1997**.
- [38] ORTEP-3 for windows: L. J. Farrugia, *J. Appl. Crystallogr.* **1997**, 30, 565.
- [39] A. L. Spek, *PLATON, Molecular Geometry Program*, University of Utrecht, The Netherlands, **1999**.

Received: May 9, 2009
Published Online: August 6, 2009